# Site-Specific Chemistry of Gallium Arsenide Metalorganic Chemical Vapor Deposition

Q. Fu, L. Li, M. J. Begarney, B.-K. Han, D. C. Law and R. F. Hicks

Chemical Engineering Department, University of California, Los Angeles, CA 90095-1592 USA

**Abstract.** Herein, we summarize our studies of the surface chemistry of gallium arsenide as it pertains to the metalorganic chemical-vapor deposition of compound semiconductors. It has been found by scanning tunneling microscopy and vibrational spectroscopy that the adsorption of reactant molecules on reconstructed GaAs (001) surfaces is "site-specific." Trimethylgallium dissociatively adsorbs only on arsenic sites, whereas arsine dissociatively adsorbs only on gallium sites. The decomposition of one precursor molecule ($Ga(CH_3)_3$ or $AsH_3$) creates the site for the decomposition of the other molecule ($AsH_3$ or $Ga(CH_3)_3$, respectively). In this fashion, the crystal grows one atomic layer at a time. Studies of carbon doping with carbon tetrachloride have shown that adsorbed chlorine attacks the exposed gallium and generates volatile $GaCl_x$ species. The site-specific nature of this reaction leads to a dramatic change in the film morphology, with the formation of 30-nm etch pits randomly distributed over the surface.

## 1. INTRODUCTION

Metalorganic chemical vapor deposition (MOCVD) is the technique of choice for fabricating III/V compound semiconductor devices. These devices have many exciting applications, including automotive radar, full-spectrum light-emitting diodes, digital wireless amplifiers and receivers, fiber-optic amplifiers, microwave devices, broadband cable modems, and satellite photovoltaics, to name a few of the fastest growing products in this field [1]. To support the growth of this technology, the science underlying the manufacturing process should be understood as thoroughly as possible. In metalorganic chemical vapor deposition, there is a confluence of several scientific fields, encompassing device physics, materials science, reactor engineering, and surface chemistry [2,3]. It is our opinion that the latter field holds the key to unlocking the full potential of the MOCVD process, and it is this area where we have focussed our energies over the past five years [4-18,32]. Some of the highlights of this research will be described in the present paper.

Most III/V semiconductor devices are grown on the (001) plane of gallium arsenide. Ideally, this plane is terminated with either a layer of gallium atoms, or a layer of arsenic atoms. However in reality, it reconstructs into many different structures, each with a unique distribution of surface sites [19]. An overriding feature of these surfaces is the formation of As-As and Ga-Ga dimers, which reduces the density of the dangling bonds and minimizes the surface free energy. In addition, rows of missing dimers are created to expose the atoms in the second layer of the crystal. This is accompanied by charge transfer between the arsenic and gallium, resulting in filled As and empty Ga dangling bonds, and a further lowering of the surface free energy [20].

Shown in Fig. 1 are ball-and-stick models for three reconstructions of gallium arsenide (001). The (m×n) designation is derived from the size of the surface unit cell relative to that of the bulk plane, where m and n are integer multiples of the (001) lattice constant in the $[\bar{1}10]$ and [110] directions. The c(4×4) structure occurs at an arsenic coverage of 1.75 monolayers (ML), and is characterized by a layer of As dimers sitting on top of a complete layer of arsenic atoms [21]. This structure and closely related variants are normally present during MOCVD [10,11,15]. At an arsenic coverage of 0.75 ML, the β2-(2x4) phase

is formed. This unit cell contains two arsenic dimers in the top layer and a third arsenic dimer in the trench. The As-dimer bond on the β2-(2x4) is rotated 90$^{o}$ relative to the As-dimer bond on the c(4x4). Lowering the arsenic coverage to 0.25 ML creates the gallium-rich (4x2) reconstruction. It contains two gallium dimers in the top layer and one gallium dimer in the trench [24]. Examination of the β2-(2x4) and (4x2) models reveals that there are four sites for the adsorption and reaction of precursor molecules: As dimers, Ga dimers, second-layer As atoms, and second-layer Ga atoms [4-5]. On the c(4x4), the arsenic dimers in the top layer already occupy all the adsorption sites, in other words, this surface is fully passivated. For other molecules to stick to the c(4x4), they must displace the As dimers first [15].

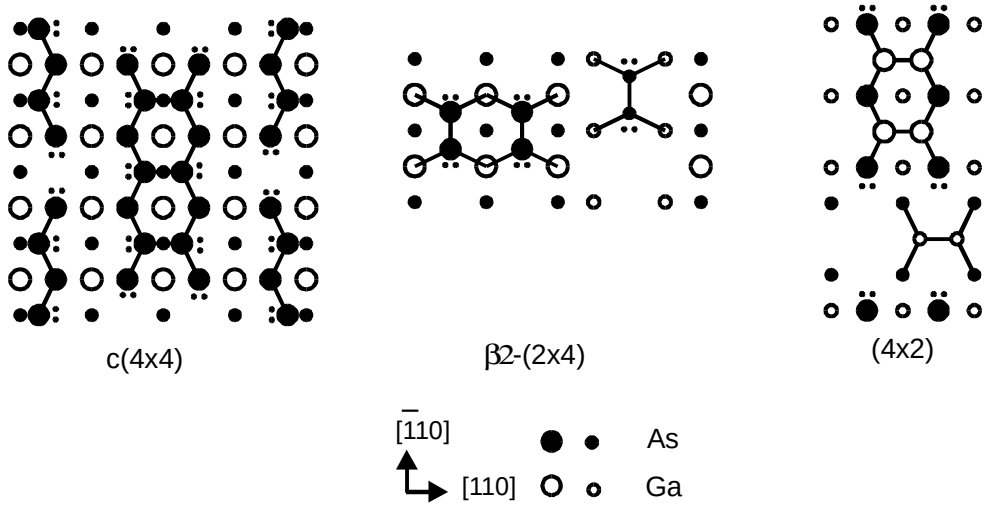


Fig. 1. Ball-and-stick models for three GaAs (001) reconstructions.

Below, we examine the adsorption and reaction of hydrogen, trimethylgallium, arsine and carbon tetrachloride on gallium arsenide (001) surfaces [6,7,9]. Hydrogen adsorption has been studied for several reasons. This gas plays a special role in promoting the consumption of the alkyl radicals, and it helps maintain a clean growth surface. Hydrogen is also the ideal probe molecule, because it adsorbs on all the dangling bonds, and from the vibrational spectrum of adsorbed hydrogen, one can determine the distribution of adsorption sites on the semiconductor surface. Trimethylgallium and arsine are of interest because they are the metalorganic reagents used for MOCVD. Carbon tetrachloride, on the other hand, is a source of p-type carbon doping of gallium arsenide. As the reader shall see, the surface reactions of these molecules are site-specific. For example, arsine adsorbs on gallium dimers, whereas trimethylgallium adsorbs on arsenic dimers. We show that in the case of carbon tetrachloride, the site-specific reaction with gallium causes a dramatic change in the GaAs film morphology.

## 2. EXPERIMENTAL APPARATUS

The experiments described in this paper were conducted in a unique apparatus that is shown in Fig. 2. It consists of a central sample server, a load-lock, two ultrahigh vacuum chambers, and a horizontal square-duct MOCVD reactor. Compound semiconductor thin films are grown in the MOCVD reactor, then transferred directly into the ultrahigh vacuum system via an interface chamber. Once there, the crystal surfaces are characterized by an array of analytical techniques, including x-ray photoemission spectroscopy (XPS), low-energy electron diffraction (LEED), thermal desorption mass spectroscopy (MS), infrared spectroscopy (IR), and scanning tunneling microscopy (STM) [12]. A detailed description of the growth procedure and the methods used to study the semiconductor surfaces are given elsewhere [12].

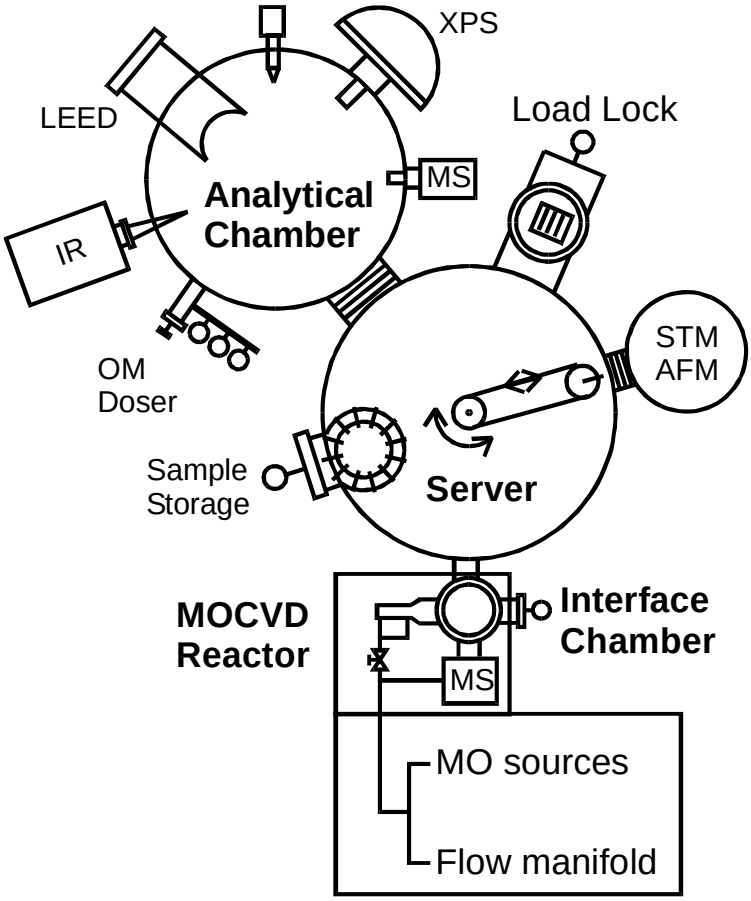


Fig. 2. Schematic of the experimental apparatus.

## 3. RESULTS AND DISCUSSION

### 3.1 Surface Sites on GaAs (001)

We first consider the c(4x4), which is the most arsenic-rich reconstruction. A scanning tunneling micrograph obtained by tunneling out of the filled surface states is presented in Fig. 3 (a). One sees a zigzag pattern of gray patches with black strips in between. The gray patches are due to the filled dangling bonds associated with short chains of arsenic dimers. If the chains are two dimers in length, the patches are square (refer to the black circle in the lower left corner of the image). Conversely, if the chains are three dimers in length, the patches are rectangular (refer to the black circle in the upper right corner of the image) [11]. The model of the c(4x4) in Fig. 1 is for the case where each chain contains three arsenic dimers and corresponds to a fully passivated surface with an As coverage of 1.75 ML. On the other hand, the STM image in Fig. 3 (a) is of a c(4x4) surface with a lower arsenic coverage. When the dimer chains are shorter, As atoms in the underlying layer become exposed and can adsorb other species, such as alkyl radicals or trimethylgallium molecules.

Shown in Fig. 3 (b) are polarized infrared reflectance spectra of hydrogen adsorbed on the c(4×4). Hydrogen atoms attack the top layer of arsenic atoms converting them into arsine molecules, then more hydrogen atoms adsorb onto the second-layer arsenic atoms [15]. The spectra shown in the figure contain a series of overlapping bands in the frequency range between 2200 and 1900 $cm^{-1}$, which can be assigned to arsenic hydrides. The As-H stretching vibrations are more intense when the light is polarized parallel

to the [$\bar{1}$10] crystal axis, consistent with adsorption onto second-layer arsenic atoms. In addition to the As-H bands, a gallium hydride stretching vibration is observed at 1865 $cm^{-1}$. This is further proof of the etching of arsenic atoms.

The infrared spectra contain a series of vibrational bands of varying frequencies because the hydrogen atoms bond to arsenic and gallium atoms in different chemical environments. Some of these are illustrated by the ball-and-stick model in Fig. 3 (c). For example, sites 1 and 2 correspond to two types of arsenic monohydrides, while site 3 corresponds to an arsenic dihydride. Sites 4 and 5 show two gallium hydrides, which differ only in the coordination spheres about the adjacent arsenic atoms.

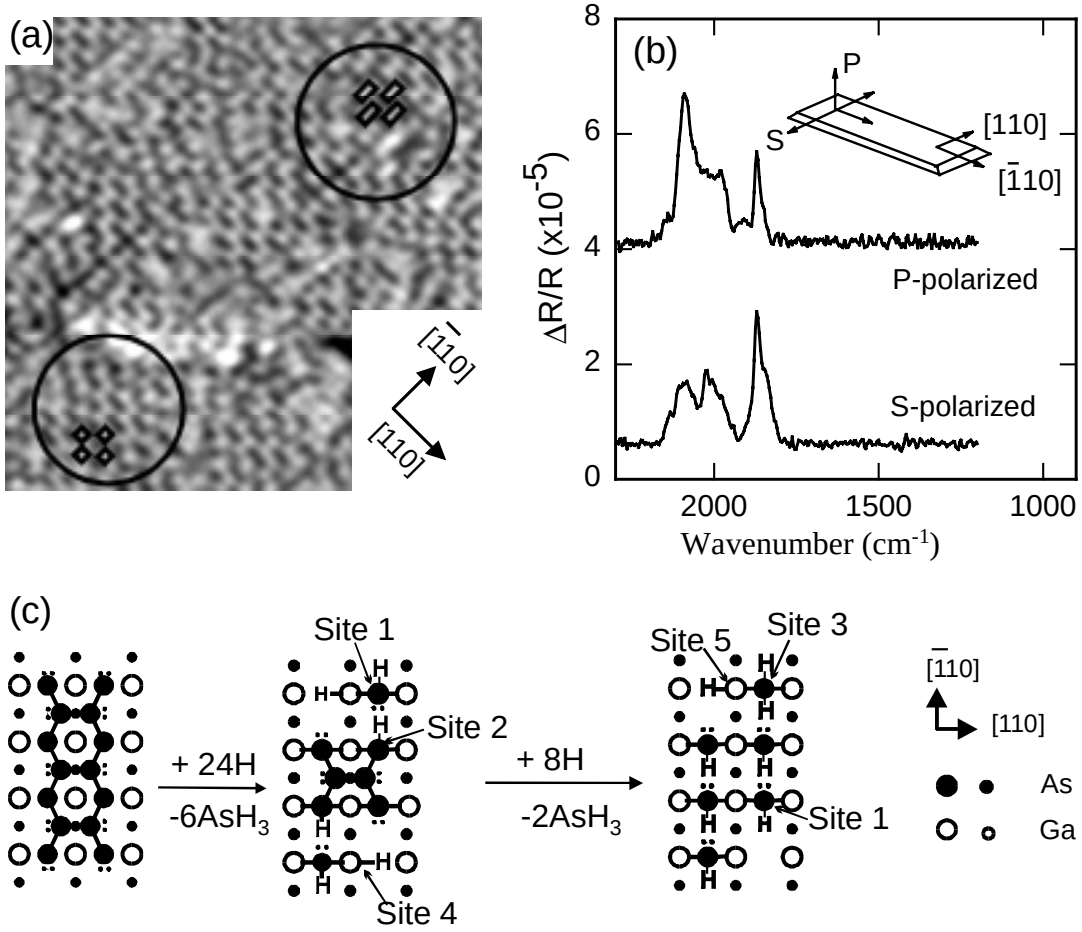


Fig. 3. Hydrogen adsorption on GaAs (001)-c(4x4): (a) fill-states STM image of the clean surface (image size 200x200 Å$^2$); (b) s- and p- polarized infrared spectra of adsorbed hydrogen and (c) ball-and-stick model.

Presented in Fig. 4 (a) is an STM image of the (2x4). A single unit cell, 8x16 Å$^2$, is highlighted by a black rectangle. The four white spots inside the rectangle correspond to the fill-states of four arsenic dangling bonds, i.e., two arsenic dimers. The dark trenches on either side of the As atoms do not provide any information on the features located there. The trenches could contain arsenic dimers, as given by the β2-(2x4) in Fig. 1, or gallium dimers, as observed for the α-(2x4) reconstruction [25]. Scanning tunneling microscopy cannot easily distinguish between these possibilities.

Shown in Fig. 4 (b) are polarized infrared spectra of hydrogen adsorbed on the (2x4) surface. The infrared spectra contain a series of bands between 2200 and 1900 $cm^{-1}$ due to arsenic hydrides, and three more bands between 1900 and 1700 $cm^{-1}$ due to gallium hydrides. Unlike the c(4x4), the top layer of arsenic atoms on the (2x4) are not etched away upon exposure to hydrogen (1800 Langmuir) [15]. The As-H vibrational bands are strongly p-polarized when the long axis of the crystal is parallel to the [$\bar{1}$10] direction, which is in the same orientation as the As-As dimer bonds. The intensities of the Ga-H vibrational bands are strongly dependent on the polarization as well, but in the opposite direction of the As-H spectra. The As-H spectra are due to arsenic monohydrides formed by hydrogen adsorption on

arsenic dimers, whereas the Ga-H peaks are due to gallium monohydrides formed by hydrogen adsorption on second-layer gallium atoms. Bands due to Ga-H-Ga bridging modes are not observed, ruling out the presence of gallium dimers in the trenches (see below). Thus, by combining infrared spectroscopy of adsorbed hydrogen with scanning tunneling microscopy, we can definitively identify the surface structure to be that of the β2-(2x4) (c.f., Fig. 1.). A model for hydrogen adsorption on this reconstruction is shown in Fig. 4 (c).

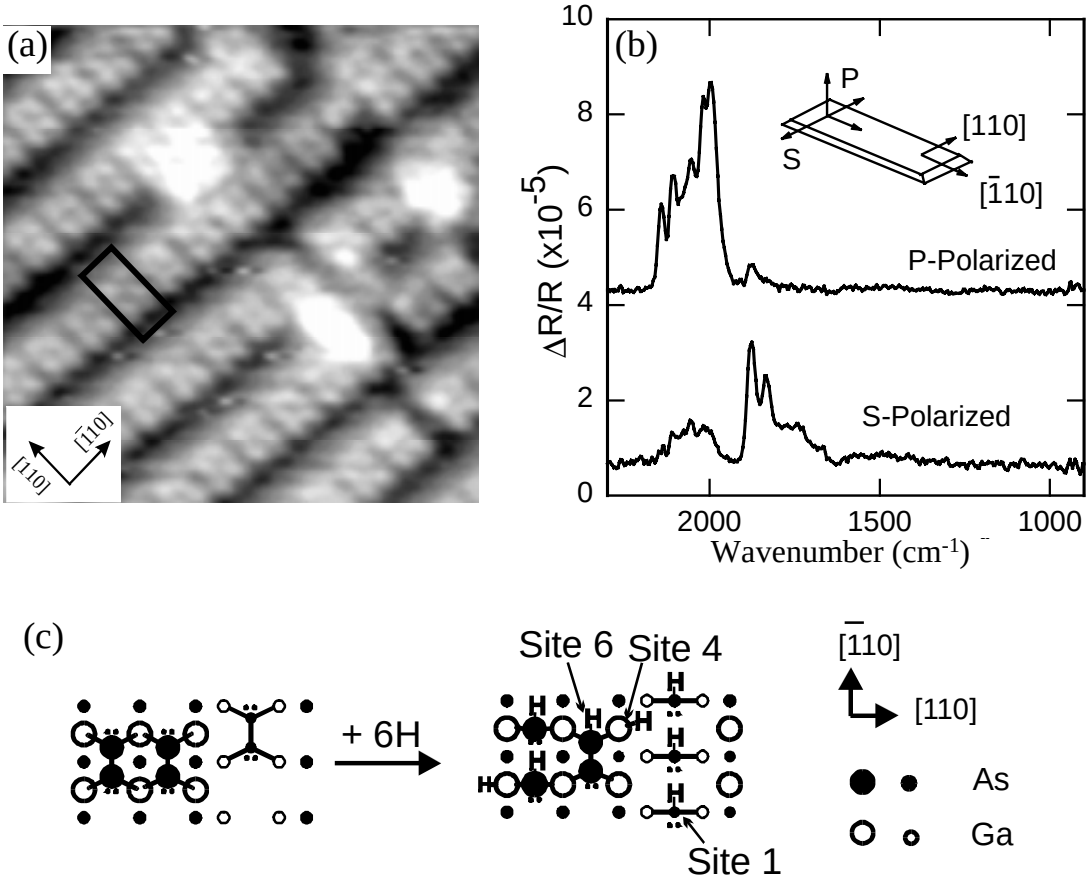


Fig. 4. Hydrogen adsorption on GaAs (001)-β(2x4): (a) fill-states STM image of the clean surface (image size 80x80 Å$^2$); (b) s- and p- polarized infrared spectra of adsorbed hydrogen and (c) ball-and-stick model for hydrogen adsorption.

A filled-states STM picture of the gallium-rich (4x2) reconstruction is presented in Fig. 5 (a). This image contains a series of double rows of light gray spots that extend along the [110] direction. The unit cell (highlighted by a black rectangle) extends for 8 Å along the rows and for 16 Å across the rows. The four gray spots seen within the rectangle arise from the lone pairs of electrons in the dangling bonds of four second-layer arsenic atoms. These lone pairs are illustrated in the ball-and-stick model of the (4x2) given in Fig. 1 (four pairs of small dots on the As atoms). If this model is correct, then one should see some evidence of gallium dimers in the STM image. It has been suggested that the bumps in the trenches between the rows are due to the Ga dimers [24]. However, a definitive assignment of these features cannot be made by inspection of the image alone.

Infrared reflectance spectra of hydrogen adsorbed on the (4x2) surface are shown in Fig. 5 (b). Between about 1950 and 950 cm$^{-1}$ a series of broad overlapping bands are seen in the s-polarized spectrum. These bands result from hydrogen adsorption on the gallium dimers, producing three-center-two-electron bonded, bridging gallium hydride [4,15,27]. The mode detected in the infrared spectrum is the asymmetric stretch, which has a dipole moment parallel to the Ga dimer bond ([110] axis). This is why the band is strictly s-polarized. The occurrence of the bridging gallium hydride provides direct experimental evidence that Ga dimers are present on the (4x2), and lends support to the model proposed for this structure in Fig. 1.

The p-polarized spectrum shown in Fig. 5 (b) contains three peaks at 2140, 2100 and 2050 $cm^{-1}$, and a shoulder at 2020 $cm^{-1}$, which are due to arsenic hydride stretching vibrations. These peaks correspond to hydrogen adsorption on second-layer As atoms and on As dimers. The second-layer As atoms occur on the (4x2), whereas the As dimers are associated with a small amount of a more arsenic-rich reconstruction (i.e., the (2x6)) that cannot be completely removed by annealing the crystal. In Fig. 5 (c), we present a model for hydrogen termination of the (4x2) surface. Again, several different sites may be distinguished from each other by their bond configuration and the coordination sphere about the Ga and As atoms. The observation of broad overlapping infrared bands between 1950 and 950 $cm^{-1}$ suggests that several bridging Ga hydrides are formed, each with a different Ga-H-Ga bond angle in the range of 95 to 120 degrees [4,15]. Ab initio calculations of gallium arsenide clusters are underway to identify the origin of each vibrational band recorded in the reflectance spectra presented in Figs. 3-5 [28].

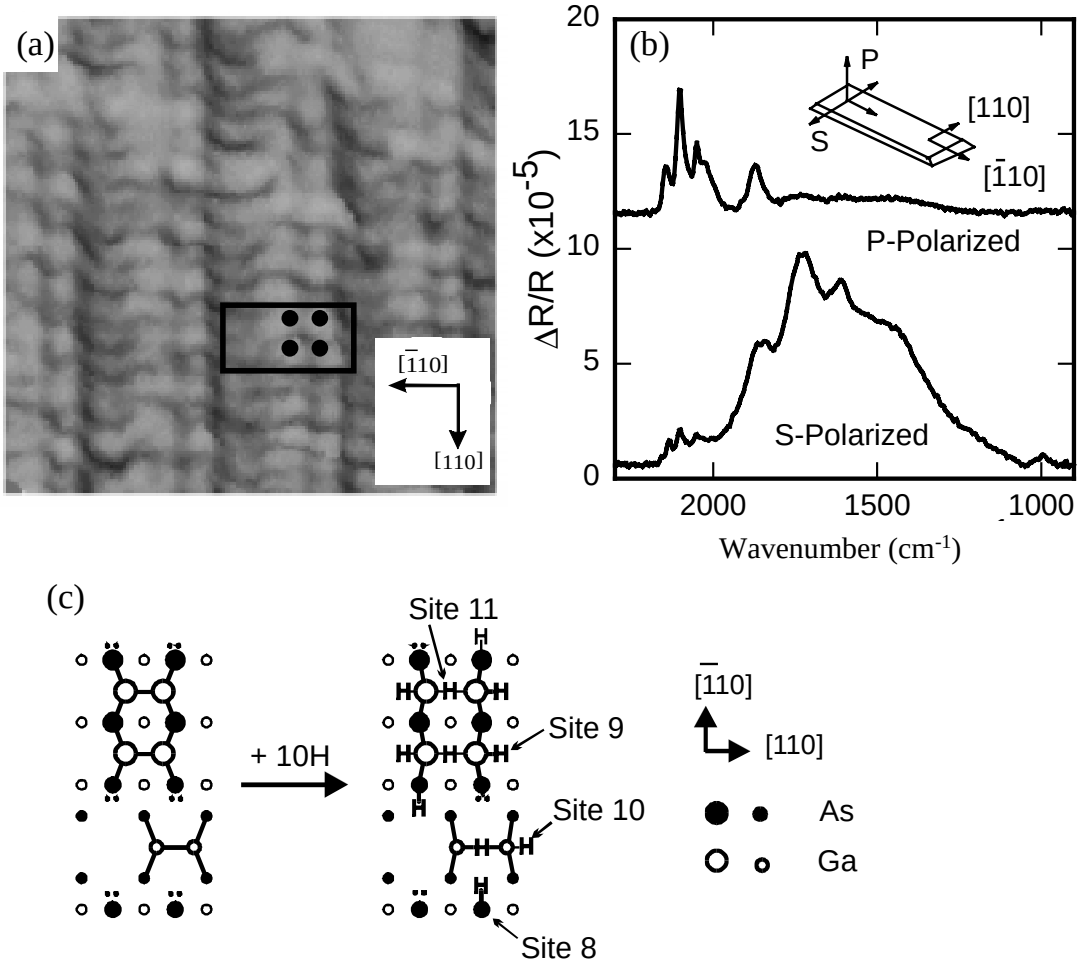


Fig. 5. Hydrogen adsorption on GaAs (001)-(4x2): (a) fill-states STM image of the clean surface (image size 60x60 $Å^2$); (b) s- and p- polarized infrared spectra of adsorbed hydrogen and (c) ball-and-stick model.

### 3.2 Surface Structure in the MOCVD Environment

The gallium arsenide surfaces described in the preceding section were prepared by depositing a thin film and annealing the crystal in ultrahigh vacuum between 673 and 873K. The question is then whether any of these structures are present during MOCVD growth. We have found that all three of these reconstructions are stable in the CVD reactor in 20 Torr of flowing hydrogen at temperatures up to 893 K [10]. However, under normal growth conditions at a mole ratio of the group V source to the group III source exceeding 10.0, a disordered c(4x4) or (1x2) phase is present [22,23]. We have characterized this surface structure by scanning tunneling microscopy and infrared spectroscopy and the results are summarized in Fig. 6 [11,18]. The filled-states STM image reveals a surface terminated with disordered

gray rows that are 8 Å apart (delineated by white lines in the picture). Since there is no structure along the row in the [$\bar{1}$10] direction, the unit cell size is (1x2).

Gentle heating of the (1x2) to about 473 K transforms it into the c(4x4) structure depicted in Fig. 3 (a). This suggests that adsorbates are giving rise to the surface disorder. To try and identify these adsorbates, we titrated the surface with deuterium atoms, and recorded the infrared reflectance spectrum of the sample before and after titration [18]. These results are shown in Fig. 6 (b). Two negative peaks are observed between 2800 and 3000 $cm^{-1}$, which are due to the asymmetric and symmetric C-H stretching vibrations of adsorbed alkyl groups. In addition, the small negative band near 2000 $cm^{-1}$ may be assigned to an As-H stretch, while the large positive bands at 1500 $cm^{-1}$ may be assigned to As-D stretches. These results show that the surface is covered with alkyls and some hydrogen in the MOCVD environment. A model of this surface is presented in Fig. 6 (c). The adsorption of As dimers on top of the underlying arsenic layer generates the x2 periodicity of the surface; whereas the disorder in the 1x direction arises from a random mixture of top-layer As dimers, second-layer As dimers, and adsorbed alkyls groups. We propose that the exposed second-layer arsenic atoms are the sites for adsorption and decomposition of the group III source, trimethylgallium. Alkyl radicals and $As_2$ or $As_4$ molecules present in the MOCVD reactor compete for these sites, and can actually inhibit the adsorption of the gallium precursor [29].

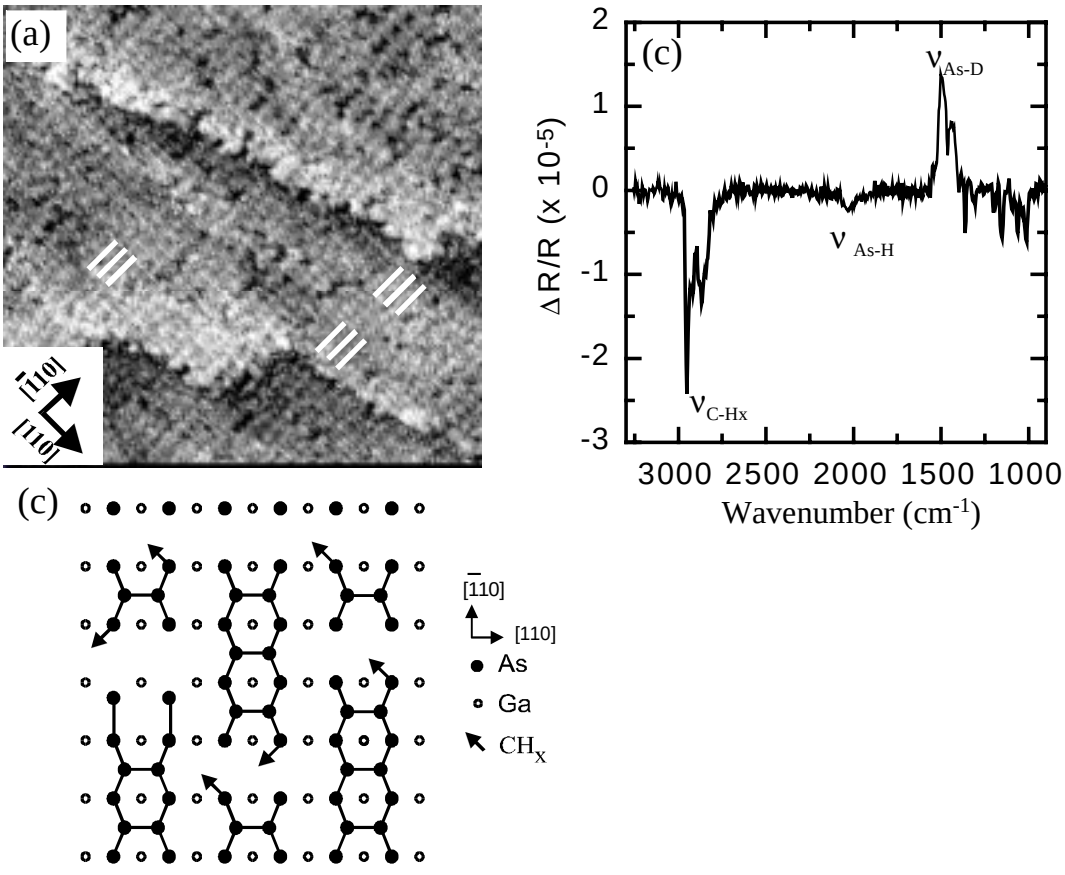


Fig. 6. (a) STM image of the GaAs (001) surface immediately after transfer from the MOCVD reactor (image size 260x260Å$^2$); (b) infrared spectrum of the surface after deuterium titration; and (c ) ball-and-stick model of the (1x2).

### 3.3 Trimethylgallium and Arsine Decomposition on GaAs (001)

We have investigated the adsorption and reaction of trimethylgallium on the β2-(2x4) surface using infrared and x-ray photoemission spectroscopy [6]. Although it would be more appropriate to study this reaction on the (1x2), the β2-(2x4) has similar adsorption sites, i.e., threefold coordinated As atoms

bound to a layer of gallium. Moreover, the latter reconstruction is much more ordered and better characterized. Presented in Fig. 7 are polarized infrared reflectance spectra of the C-H stretching vibrations arising from adsorbed trimethylgallium. Two bands are seen at about 2960 and 2880 $cm^{-1}$ due to the asymmetric and symmetric C-H stretches. The dipole moment of the latter mode is parallel to the metal-carbon bond. Therefore, if this band is polarized along the [110] direction it suggests that the methyl group is bound to gallium, whereas if this band is polarized along the $[\bar{1}10]$ direction it suggests that the methyl group is bound to arsenic. Careful inspection of the figure reveals that there are two symmetric stretching bands at about the same frequency, but with opposite polarization. The band polarized along the [110] is about twice as intense as the one polarized along the $[\bar{1}10]$.

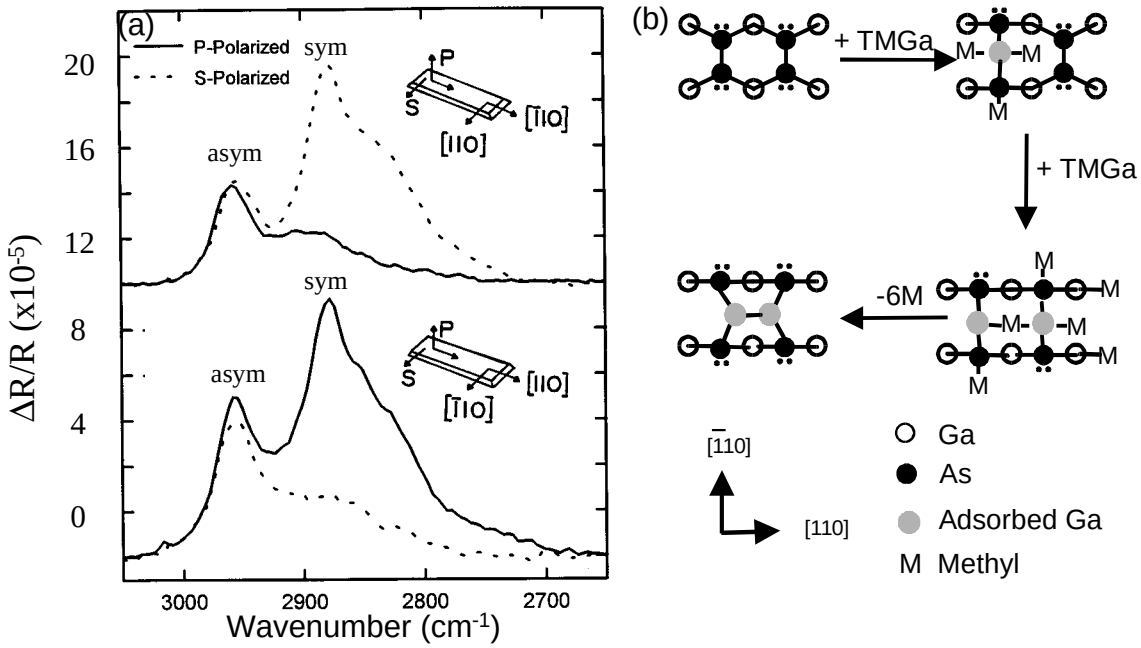


Fig. 7. Trimethylgallium adsorption on GaAs (001)-(2x4) at 310K: (a) infrared spectra of C-H stretching vibrations; and (b) ball-and-stick model for TMGa decomposition on As dimers.

The above results can be interpreted by the adsorption model presented in Fig. 7 (b). In the first reaction, a trimethylgallium molecule dissociatively adsorbs across an arsenic dimer, and transfers one of three methyl groups to the adjoining arsenic atom [6]. This configuration has been shown by theoretical calculations to be the most stable adsorbate structure on GaAs (001) [30]. Adsorption of another trimethylgallium molecule on the neighboring arsenic dimer produces the second proposed structure in Fig. 7 (b). In this case, some of the methyl ligands migrate to exposed gallium in the second-layer, and one methyl group forms a bridge bond between the two adsorbed Ga atoms. Desorption of methyl radicals from the surface (at MOCVD growth temperatures) converts the adsorbed Ga atoms into a Ga dimer [30].

Gallium dimers or adatoms produced by the reaction of trimethylgallium with an arsenic-rich surface can serve as the sites for the adsorption and decomposition of arsine. Consequently, we examined the reaction of arsine with gallium-rich GaAs (001) surfaces [7,17]. Shown in Fig. 8 (a) are polarized infrared spectra of the adsorbed arsine on the (4x2) at 298 K. Only As-H vibrations at 2135, 2100, 2090 and 2020 $cm^{-1}$ are observed; no Ga-H vibrations are present. These and other STM results we have obtained show conclusively that the arsine molecule dissociatively adsorbs on the gallium dimers, and transfers one or two hydrogen atoms to neighboring arsenic sites [17]. This reaction is illustrated by the ball-and-stick models provided in Fig. 8 (b). Following hydrogen desorption, the arsenic adatoms should dimerize, converting the surface back into an arsenic-rich reconstruction (e.g., the (1x2) or (2x4)). By combining the models presented in Figs. 7 (b) and 8 (b), one creates a complete reaction cycle for gallium arsenide crystal growth.

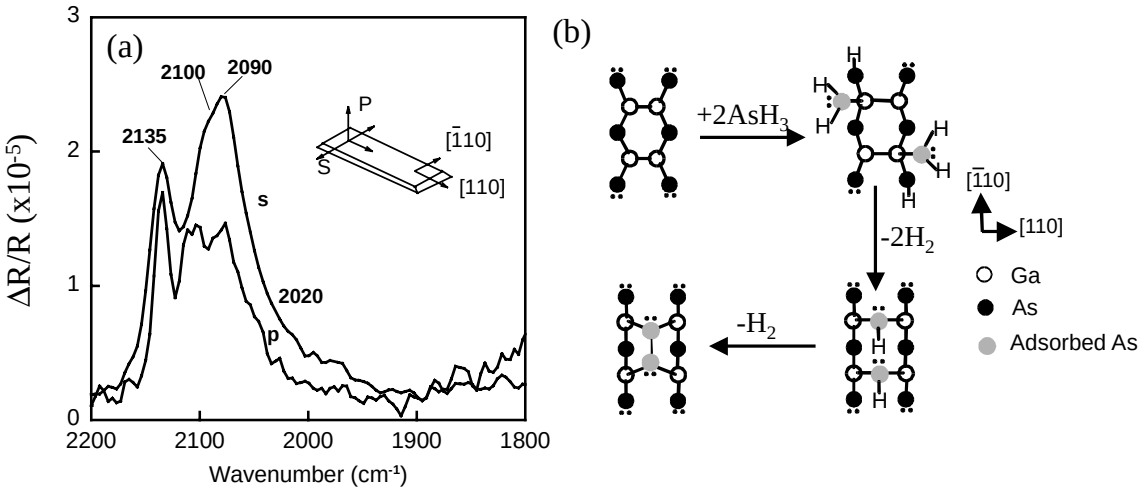


Fig. 8. Arsine adsorption on GaAs (001)-(4x2) at 300K: (a) infrared spectra of As-H stretching vibrations; and (b) ball-and-stick model for $AsH_3$ decomposition on Ga dimers.

### 3.4 Carbon Tetrachloride Decomposition on GaAs (001)

Carbon tetrachloride is an efficient source for p-type carbon doping of gallium arsenide films [16,31]. The surface reactions of this dopant molecule are complex and strongly impact the MOCVD growth process. Carbon tetrachloride decomposes on the GaAs (001) surface by two competing pathways [9,13,16]:

$$CCl_4 + 4Ga_a \rightarrow 4GaCl + C_a, \quad (1)$$

$$3CCl_4 + 4GaAs \rightarrow 4GaCl_3 + 2As_2 + 3C_a, \quad (2)$$

Equation (1) and (2) represent overall decomposition processes, and are not intended to show the mechanism, which involves a sequence of elementary steps, including adsorption, surface reaction and desorption. In the first reaction, adsorbed chlorine and gallium react with each other to desorb gallium monochloride. This causes a reduction in the GaAs growth rate that is proportional to the amount of carbon tetrachloride fed to the reactor. The second reaction becomes significant at higher concentrations of $CCl_4$ (IV/III ratios above 2.5 at 773 to 823 K) and generates gallium trichloride as the volatile product. This latter process results in anisotropic etching of the gallium arsenide film.

The adsorption of carbon tetrachloride on GaAs (001) is site-specific. In Fig. 9 (a), we present infrared spectra of adsorbed hydrogen on the (4x2) reconstruction [14]. These spectra were recorded of the clean surface and after dosing the sample with carbon tetrachloride at 300 and 473 K. Before $CCl_4$ adsorption, one sees the broad low-frequency bands between 1900 and 950 $cm^{-1}$ that are characteristic of bridge-bonded H atoms on Ga dimers. These bands decrease in intensity following $CCl_4$ adsorption at 300 K and are completely absent after exposure to the dopant molecule at 473 K. These results demonstrate that the chlorine ligands from carbon tetrachloride react with the gallium dimers, and completely remove them from the surface when this reaction is carried out about 473 K [9]

A scanning tunneling micrograph of the (4x2) surface after exposure to carbon tetrachloride at 673 K is shown in Fig. 9 (b). The reaction of chlorine with gallium causes two changes in the surface structure. First, the terraces have been converted from the (4x2) into a (3x2) reconstruction, with a corresponding increase in the As coverage from 0.25 to 0.33 ML. Secondly, etch pits form along the step edges that are up to six atomic layers deep. Within these pits, the surface has reconstructed into the (2x4) phase with an arsenic coverage of 0.75 ML [14]. The two changes seen in the STM image illustrate the two competing reaction pathways: equation (1), which consumes adsorbed gallium; and equation (2), which etches the gallium arsenide film.

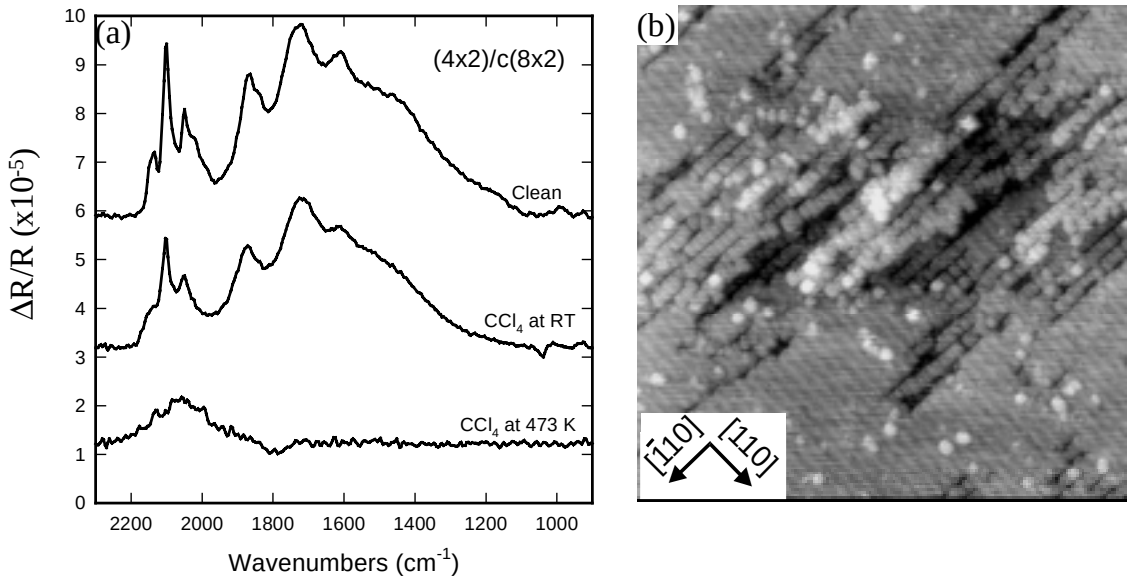


Fig. 9. Carbon tetrachloride adsorption on GaAs (001)-(4x2): (a) infrared spectra of hydrogen titration of adsorbed $CCl_4$ and (b) STM image of surface after $CCl_4$ adsorption at 473 K and heating to 673 K (image size 1200x1200 Å$^2$).

The gallium arsenide etching reaction is further manifest in the nano-scale features of the film [16]. Shown in Fig. 10 is an STM picture of a surface after the deposition of 0.1 microns of GaAs at 818 K, 20 Torr $H_2$, 10 ppm triisobutylgallium, a V/III ratio of 30.0 (V = tertiarybutylarsine), and a IV/III ratio of 5.0. In the image, one sees a series of smooth terraces, on average about 1000 Å across, that are separated by steps two atomic layers in height. Randomly distributed over the surface, but located at the step edges, are circular pits approximately 300 Å in diameter. These pits evolve from the features seen in the atomic-scale STM image in Fig. 9 (b). They occur when the amount of adsorbed chlorine greatly exceeds that of the adsorbed gallium. The site-specific nature of the etching reaction leads to pit formation. The high

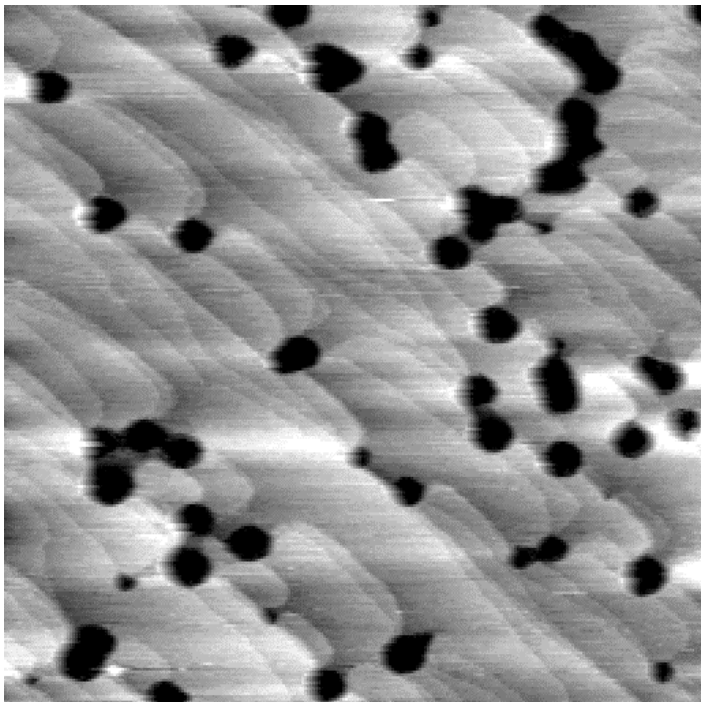

Fig. 10. Etch pits on (001) surface produced by $CCl_4$ decomposition during MOCVD of GaAs (image size 1.5x1.5 μm$^2$).

density of steps within the pits exposes gallium atoms to chlorine, whereas none of these Ga sites are present on the c(4x4) or (1x2) terminated terraces. Consequently, the etching reaction is localized to the pit surface.

## 4. CONCLUDING REMARKS

In this paper, we hope to have convinced the reader that the MOCVD of compound semiconductors occurs through a series of surface reactions that are site specific. This phenomenon arises because of the substantially different chemical reactivities of the group III and V elements, i.e., the arsenic and gallium dimers. In the future, we intend to explore the surface chemistry of MOCVD further. For example, more work is needed to identify the reaction sites on the GaAs (001)-(1x2) structure that is present during growth at high V/III ratios. Moreover, we are quite interested in the surface chemistry of the MOCVD of indium phosphide and related materials. These semiconductors here have hardly been investigated. Studies of InP film growth should yield a number of surprises, given that the InP surface exhibits entirely different structures from those observed on GaAs [32].

**Acknowledgements**

Funding for this research was provided by the Office of Naval Research (N00014-95-1-0904), and by the National Science Foundation, Chemical and Thermal Systems (CTS-9531785) and Division of Materials Research (DMR-9804719).

**References**

[1] Whitaker T., and Meyer M., *Compound Semiconductors* **5** (1999) 25-40.
[2] Stringfellow G.B. Organometallic Vapor-Phase Epitaxy: Theory and Practice (Academic Press, 1989).
[3] Hitchman M. L., and Jensen K. F., Chemical Vapor Deposition: Principles and Applications (Academic Press, 1993).
[4] Qi H., Gee P. E., and Hicks R. F., *Phys. Rev. Lett.* **72** (1994) 250-253.
[5] Qi H., Gee P. E., Nguyen T., and Hicks R. F., *Surf. Sci.* **323** (1995) 6-18.
[6] Gee P. E., Qi H., and Hicks R. F., *Surf. Sci.* **330** (1995) 135-146.
[7] Qi H., Gee P. E., and Hicks R. F., *Surf. Sci.* **347** (1996) 289-302.
[8] Adamson S.D., Han B.-K., and Hicks R.F., *Appl. Phys. Lett.*, **69** (1996) 3236-3238.
[9] Li L., Gan S., Han B.-K., Qi H, and Hicks R. F., *Appl. Phys. Lett.* **72** (1998) 951-953.
[10] Li L., Han B.-K., and Hicks R.F., *Appl. Phys. Lett.* **73** (1998) 1239-1241.
[11] Han B. K., Li L., Fu Q., and Hicks R. F., *Appl. Phys. Lett.* **72** (1998) 3347-3349.
[12] Li L., Han B.-K., Gan S., Qi H., and Hicks R. F., *Surf. Sci.* **398** (1998) 386-394.
[13] Begarney M.J., Warddrip, M.L., Kappers, M.J., and Hicks, R.F., *J. Cryst. Growth **193** (1998) 305-315.*
[14] Li L., Qi H., Gan S., Han B. -K., and Hicks R. F., *Appl. Phys. A* **66** (1998) S501-505.
[15] Hicks R. F., Qi H., Fu Q., Han B.-K., and Li L., *J. Chem. Phys.* 1999 (in press).
[16] Begarney M.J., Li L., Han B.-K., Law D.C., Li C., Yoon H., Goorsky M.S., and Hicks R. F., *J. Appl. Phys.* (1999) (in press).
[17] Fu Q., Li L., Li C., Han B.-K., Law D.C., Begarney M.J., and Hicks R.F., *Surf. Sci.* (1999) (submitted).
[18] Han B.-K. Li L., Begarney M. J., Law D., Fu Q., and R. F. Hicks, *J. Electro. Chem. Soc.* (1999) (in press).
[19] Duke C. B., Appl. *Surf. Sci*. **66** (1993) 543-52.
[20] Pashley M. D., *Phys. Rev. B* **40** (1989) 10481-10487.

[21] Biegelsen D. K., Bringans R. D., Northrup J. E., and Swartz L. E., *Phys. Rev. B* **41** (1990) 5701-5706.
[22] Kamiya I., Tanaka H., Aspnes D.E., Koza M., and Bhat R., *Appl. Phys. Lett.* **63** (1993) 3206-3208.
[23] Kamiya I., Aspnes D.E., Florez L.T., and Harbison J.P., *Phys Rev B (Condensed Matter)*, **46** (1992) 15894-904.
[24] Hashizume T., Xue Q. K., Ichimiya A., and Sakurai T., *Phys. Rev. B* **51** (1995) 4200-4212; Xue Q. K.; Hashizume T., Zhou J. M., Sakata T., Sakurai T., and Ohno T., *Phys. Rev. Lett.* **74** (1995) 3177-3180.
[25] Farrell H. H., and Palmstron C. J., *J. Vac. Sci. Technol. B* **8** (1990) 903-907.
[26] Stroscio J. A. and Kaiser W J. Eds. Scanning Tunneling Microscopy (Methods of Experimental Physics, Vol 27) (Academic press, 1994).
[27] Pulham C. R., Downs A. J., Goode M. J., Rankin D. W. H., and Robertson H. E., *J. Am. Chem. Soc*. **113** (1991) 5149-5162.
[28] Hicks R. F. (1999) (unpublished results).
[29] Ingle N.K., Theodoropoulos C., Mountziaris T.J., Wexler R.M., and Smith, F.T.J., *J. Cryst. Growth* **167** (1996) 543-556.
[30] Goringe C.M., Clark L.J., Lee M. H., Payne M.C., Stich I., White J.A., Gillan M.J., Sutton A.P., *J. Phys. Chem.* B **101** (1997) 1498-1509.
[31] Stockman S.A., Hanson A.W., Lichtenthal S.M., Fresina M.T., Hofler G.E., Hsieh K.C., and Stillman G.E., *J. Electron. Mater*. **21** (1992) 1111-1118.
[32] Li L., Han B.-K., Fu Q., and Hicks R.F., *Phys. Rev Lett.* **82** (1999) 1879-1882.